IS DENSITY FLOW BALANCING THE SALT BUDGET OF THE OKAVANGO DELTA? EVIDENCE FROM FIELD AND MODELLING STUDIES

Peter BAUER, **Stephanie ZIMMERMANN**, **Rudolf HELD**, **Thomas GUMBRICHT** and **Wolfgang KINZELBACH**

Institute of Hydromechanics and Water Resources Management,
ETH Hoenggerberg, 8093 Zürich, SWITZERLAND; bauer@ihw.baug.ethz.ch

ABSTRACT

In this paper, the salt balance of the Okavango Delta in Botswana is assessed. Large-scale arguments are presented that show the crucial role of the wetland/dryland interface for balancing the salt budget. On the other hand, modelling and field studies on selected islands are presented. Modelling results indicate a potentially unstable vertical concentration distribution below the islands. Results from TEM soundings and groundwater surveys clearly show strong conductivity anomalies for the islands. However, the data are still insufficient to prove the occurrence of density driven flow in the Okavango Delta.

INTRODUCTION

In northern Botswana, the Okavango River forms a huge wetland system called the Okavango Delta (Figure 1). Sedimentation into a graben structure that is connected to the East African Rift Valley has built up this large alluvial fan. The waters of the Okavango River originate in the humid tropical highlands of Angola, flow southward into the Kalahari basin and spill out in the Okavango Delta. A large fraction (>90%) of the inflowing water in the Delta is lost to the atmosphere via evapotranspiration. Nevertheless, the surface water in the wetland stays fresh with solute concentrations roughly tripling from the inlet to the outlet. Mass balance calculations indicate that some 300'000 tons of solutes are thus accumulated in the Delta every year. This in turn suggests, that 30% of the water lost to the atmosphere is not evaporated or transpired from the wetland water surface, but infiltrated into the shallow sand aquifers of the surrounding islands and drylands. There, the salt is left behind, forming highly concentrated brines and efflorescent crusts that can be also seen from satellite and aerial imagery. The interface between floodplains and drylands is therefore the place, where most of the salt is accumulated and potentially vertical downward flow may be triggered by density differences in the aquifer. The high salinity of the deep groundwater underlying the Okavango Delta seems to support the hypothesis that eventually, the salt input is transported vertically into the deep subsurface. Instead of a spatially homogenous increase in concentrations, the system produces a pattern of "hot spot salinization" that can exhibit, locally, the extremely high concentration gradients needed for density driven flow to take place. An essential prerequisite for this process is the complex pattern of floodplains, channels and islands of varying size observed in the Delta.

The key role of islands with respect to the salt balance of the Okavango Delta has been stressed by several authors (e.g. McCarthy and Ellery, 1994). In this paper, small-scale evidence from detailed field studies on several islands are combined with large-scale knowledge and data derived from satellite imagery. This yields new insights into the salt balance of the Okavango Delta.

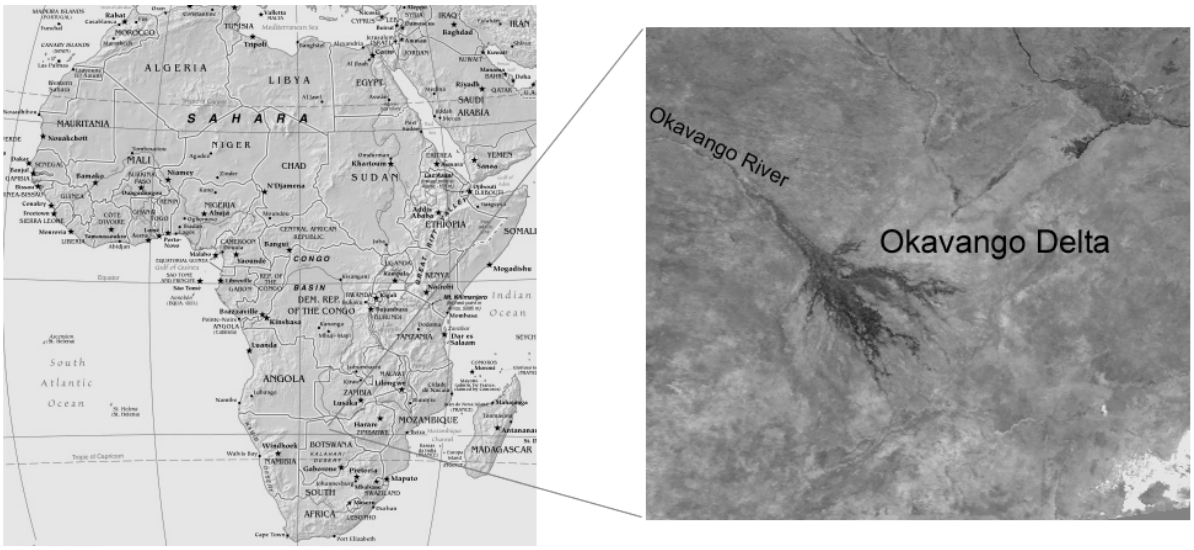

Figure 1 *Location of the Okavango Delta*

LARGE-SCALE SALT BALANCE IN THE OKAVANGO DELTA

The mean discharge of the Okavango River at Mohembo at the top of the panhandle is 300 $m^3 s^{-1}$. The inflowing water has an average TDS concentration of 35 gm^{-3}. Practically all the inflowing water is lost to evapotranspiration during the passage of the Delta and only around 7.5 m^3s^{-1} leave the Delta via the Thamalakane outflow. That water has a TDS concentration of 95 gm^{-3} (McCarthy and Ellery, 1994). Annual rainfall in the region is of order 500 mma^{-1} and typical TDS concentration in the rainfall is around 5 gm^{-3} (Gieske, 1992). Assuming an average swamp size of 10'000 km^2, the salt input by precipitation amounts to 25'000 tons per year and is thus one order of magnitude less than the salt input via the Okavango River. Calculating a simple box mass balance from these figures, indicates that approximately 10 kgs^{-1} of salts accumulate in the Delta, which is equivalent to 300'000 tons per year.

Let us consider the surface water body of the Okavango Delta as a uniform well mixed box, having the TDS concentration of the outflow, namely 95 gm^{-3}. Water is evaporated from this water body and transpired by aquatic plants. At the same time, water infiltrates into the shallow aquifers around the swamps, feeding a fringe of lush vegetation. Assuming that the surface water box is in steady state with respect to TDS concentration and well mixed, we can set up the following mass balance equation:

$$Q_{in} \cdot c_{in} = Q_{out} \cdot c_{box} + Q_{\inf} \cdot c_{box} \qquad (1)$$

Q_{in} is the inflow and c_{in} the TDS concentration in the inflow. Q_{out} is the outflow, Q_{inf} is the infiltration flux into the shallow aquifers and c_{box} is the TDS concentration in the well-mixed box representing the surface water body. Salt input by precipitation is neglected. From this balance equation, the infiltration flux can be estimated to be in the order of 100 m^3s^{-1}. Thus, roughly 60% of the inflow would be evaporated or transpired from the open water surface, whereas about 30% infiltrate into the shallow aquifers. In the long-term average, the flooded surface of the Okavango Delta is approximately 6000 km^2 (McCarthy et al., 2002). The net exchange from the flooded surface (Precipitation-Evapotranspiration) is therefore 3.3 $\cdot 10^{-8}$ ms^{-1}. This value corresponds well to the value of 3.0 10^{-8} ms^{-1} derived for the net exchange by Bauer et al. (2002) from remote sensing data.

To further elaborate on the salt balance, a simple conceptual model for the interface between swamp and islands/drylands is introduced. The swamp may be considered embedded into an unconfined aquifer and the water table in this aquifer is determined by the fixed head in the swamp and the evapotranspiration function (ET) in the dryland. A linear dependence of ET from water level depth is assumed in the common form

$$ET(h) = ET_{\max}\left(1 - \frac{S-h}{d_{ex}}\right) \quad (2)$$

where S is the land surface elevation (m) and d_{ex} is the extinction depth (m). ET_{max} is the maximum evapotranspiration rate (ms^{-1}), occurring at a water level at or above the land surface. h is the hydraulic head (m). Using this evapotranspiration formulation in the standard steady-state 1D groundwater flow equation yields the following differential equation for hydraulic head:

$$T\frac{d^2h}{dx^2} = ET_{\max}\left(1 - \frac{S-h}{d_{ex}}\right) \quad (3)$$

T is the transmissivity (m^2s^{-1}). Solving the equation subject to h(0)=H yields

$$h(x) = (H - S + d_{ex})\exp\left(-\sqrt{\frac{ET_{\max}}{d_{ex}T}}\,x\right) + S - d_{ex} \quad (4)$$

From Equation 4, the form of the water table is governed by a horizontal "ET-penetration" distance of

$$\sqrt{\frac{d_{ex}T}{ET_{\max}}}$$

This analytical expression for the water table away from the swamp can now be used to calculate an integral water loss *I* per unit length of swamp/dryland interface, as $I = \int_0^\infty \left(1 - \frac{S-h}{d_{ex}}\right) ET_{\max}\,dx$.

We obtain:
$$I = \frac{(H - S + d_{ex})}{d_{ex}}\sqrt{ET_{\max}\,d_{ex}\,T} \quad (5)$$

Hence *I* (m^2s^{-1}) represents the amount of water sucked into the dryland aquifer. With the estimated amount of infiltrating water, Q_{inf}, we can now give an order of magnitude estimate of the required length of swamp/dryland interface that should be present in the Delta:

$$L_{DW} = \frac{Q_{\inf}}{I} \quad (6)$$

With typical values of 10^{-8} ms^{-1} for ET_{max}, 20 m for d_{ex} and 10^{-3} m^2s^{-1} for T, we derive L_{DW} in the order of 7000 km.

The actual length of the wetland/dryland interface in the Okavango Delta was quantified from an island database (Gumbricht et al., 2002). The island database was obtained by vectorization of a land cover map that was, in turn, created by a combination of satellite data sources. The resulting interface length is shown to be a function of the included minimum island size; i.e. displays fractal scaling. For example, including all islands of an equivalent radius of greater than 100 m forms a wetland/dryland interface of about 7000 km (see Gumbricht et al., 2002). Thus, the above estimated interface length required for the salt balance would be available in the Okavango Delta.

With respect to the vertical flow pattern below islands, three distinct patterns may be hypothesized: (1) Dominantly upward flow. The salt is accumulating below the island; concentrations are constantly rising until saturation occurs. Salt precipitation processes below the island exist indeed and are well studied by McCarthy and co-workers (e.g. McCarthy and Ellery, 1994). Only less soluble salts such as

calcite and amorphous silica precipitate, whereas highly soluble salts do not reach saturation. (2) A downward vertical density gradient is building up, while the salt is accumulating and precipitating below the islands. However, as long as the evapotranspiration is high, the stabilizing effect of the upward flux inhibits vertical density driven flow. The stability number governing the problem (Wooding, 1960), does not reach the critical value within the life cycle of the island. It is only when the regional flooding pattern changes and the surrounding swamps fall dry that a decrease in the evapotranspiration rate allows vertically downward flow; (3) Dominantly downward flow. Salt concentration is building up below the island to the point, where the critical Wooding number is reached. From that time on, density driven vertical flow takes place.

TRANSPORT PROCESSES BELOW THE ISLANDS

Advective-dispersive transport

Let us consider the simple conceptual model of an island surrounded by swamps. In a first step, only advective-dispersive salt transport may be considered. The salt is transported into the island with the inflowing water and below the island occurs dispersive mixing. If vertical mixing is fast compared to the other transport processes, one can treat the island as a horizontal 1D problem with constant aquifer thickness. This will be done in this section in order to derive exact solutions that allow for order of magnitude estimates. The more complex 2D situation is treated numerically in the subsequent section of this paper.

The average size of an Okavango island is relatively small and therefore the evaporative drawdown below the island will always be much smaller than the ET extinction depth. Thus, setting the ET rate constant for the entire island seems an appropriate approximation. For reasons of simplicity, we treat the mass transport equation for an infinitely elongated island. The mass transport equation for such an island reads

$$\frac{\partial c}{\partial t} = D\frac{\partial^2 c}{\partial x^2} + \frac{ET}{n\,m}\,x\,\frac{\partial c}{\partial x} + \frac{ET}{n\,m}\,c \qquad (7)$$

D is the dispersion coefficient (m^2s^{-1}), n is the porosity and c is the TDS concentration (gm^{-3}). Solving this equation for steady state conditions yields

$$c(x) = C_F \exp\left(\frac{ET}{2n\,D\,m}\left(L^2 - x^2\right)\right) \qquad (8)$$

where L (m) is the half-width of the island. Usually, in the Okavango Delta, a factor of up to 1000 between the TDS concentration in the swamp and the TDS concentration in the centre of the island is observed. From Equation 8 we calculate this factor as

$$\frac{c_{\max}}{C_F} = \exp\left(\frac{ET}{2n\,D\,m}\,L^2\right) \qquad (9)$$

For a typical island, Equation 9 yields a factor of 22000 (with $D=10^{-5}$ m^2s^{-1} and n=0.2), which is much higher than observed in the field. The transient solution for Equation 7 indicates that the time scale for the build-up of such concentrations in the centre is extremely long (of order thousands of years). We conclude, that only smaller islands can be in an advective-dispersive steady state, with respect to the TDS concentration.

As explanation for the observed lower TDS concentrations, we propose an additional process holding the TDS concentrations in the centre of the islands far below the advective-dispersive steady state value. We suggest that this process may be density driven vertical flow. The salt that is removed from

the shallow layer is disposed in the deep aquifer units, which are generally saline in the Okavango Delta region.

Density Driven Flow and Stability Analysis

The coupling between flow and transport in variable density flow problems leads to non-linear differential equations that can exhibit complex behaviour in time and space. If a small perturbation is applied to an unstable solution of the governing differential equations, that disturbance will not be damped but will grow in time and lead to density driven fingering. Wooding (1960) carried out a stability analysis for a problem of variable density flow that is quite similar to ours. His analysis yields interesting insights to the functioning of the Okavango islands.

Wooding (1960) assumed the fluid density as a function of the vertical coordinate only and independent of x and y:

$$\rho(z) = \rho_0 + (\rho_1 - \rho_0)\,\exp\left(\frac{u\,z}{D}\right) \tag{10}$$

where ρ_0 is the fluid density at $z = -\infty$ and ρ_1 is the fluid density at the upper boundary of the flow domain at $z = 0$. u is the uniform fluid flow velocity directed vertically upwards and D is the diffusion/dispersion coefficient. The Raleigh-Number governing this problem (Wooding-Number) is derived as:

$$\lambda = \frac{(\rho_1 - \rho_0)\,k_f}{\rho_0} \tag{11}$$

The critical Wooding-number, i.e. the condition for the onset of instability, is a function of the wavelength of the applied disturbance. Density driven vertical flow can only be expected for a Wooding number above 7.0 (Wooding, 1960). Once the critical Wooding number is reached, density flow may be triggered. Consequently, for the Okavango island, there would be a two-phase life cycle consisting of an accumulation phase, in which the Wooding number is still sub-critical followed by a fingering phase in which density fingering occurs and vertical downward flow takes place.

MODELLING STUDIES

A typical Okavango Delta island was modelled using the finite-difference groundwater code MODFLOW (Macdonald and Harbaugh, 1988) and the transport code MT3DMS (Zheng and Wang, 1999) without density considerations. Variable density calculations were carried out with the SEAWAT model (Guo and Langevin, 2002), which is built on MODFLOW and MT3DMS. Table 1 shows the simulation parameters. First, the model was run without density coupling, with results shown in Figure 2. The salt is just accumulating in the upper layer of the island.

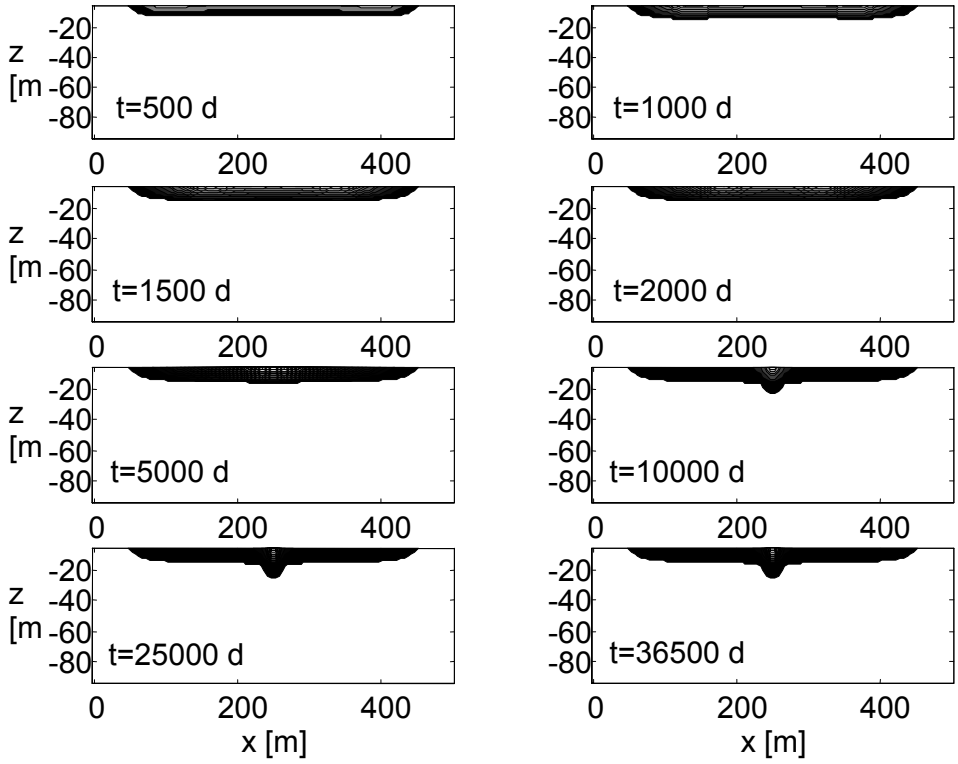

Figure 2 *Concentration iso-lines modelled without density coupling*

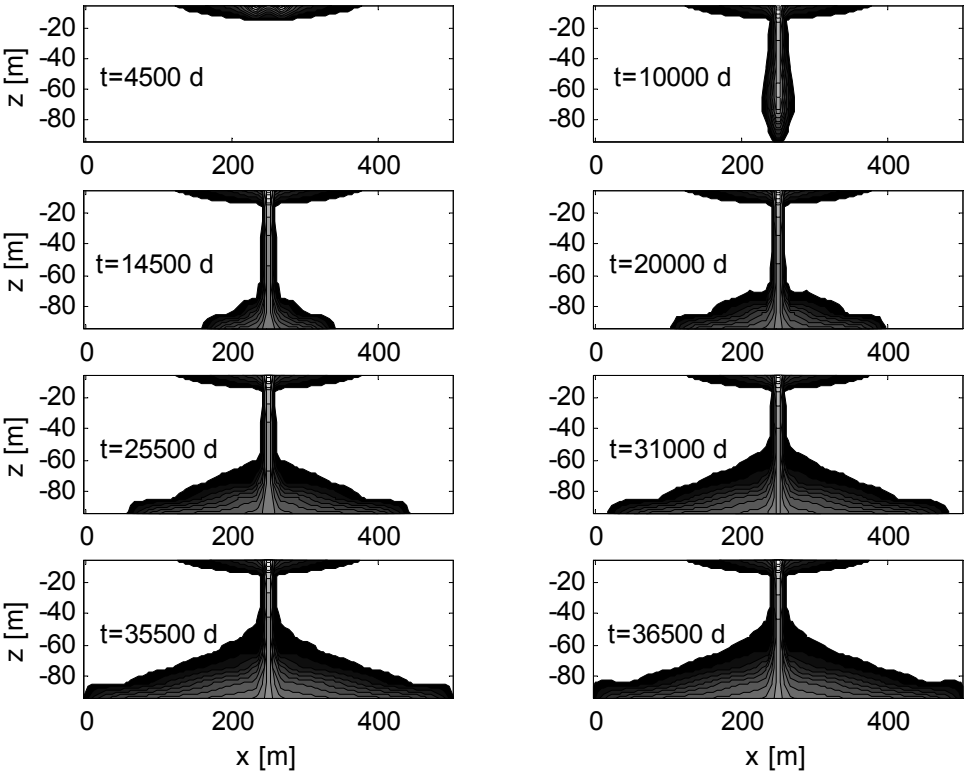

Figure 3 *Concentration iso-lines modelled with density coupling*

Island width	500m
Island thickness	100 m
Horizontal cell size	5 m
Vertical cell size	10 m
Horizontal k_f	10^{-4} ms^{-1}
Vertical k_f	10^{-5} ms^{-1}
Fixed concentration in upper corner	0,2 kgm^{-3}
Fixed head in upper corners	100 m
ET-rate	5,8 10^{-8} ms^{-1}
Effective diffusion coefficient	1,2 10^{-8} m^2s^{-1}
Porosity	0,2

Table 1 *Model Parameters for an Okavango Delta Island*

At greater depth, the concentration remains practically unaltered over the entire simulation period of 100 years. At early times, the concentration maximum is not located in the centre, but two maxima are observed, one in both halves of the island. Those maxima are travelling slowly towards the centre until they merge into one global concentration maximum in the centre of the island. Thereafter, the central concentration grows linearly in time and unrealistically high values are predicted.

Considering the effect of density in the coupling of flow and transport, the picture is dramatically changed (Figure 3). At early times, the results are quite similar, as density effects are still small. After 30 years of salt accumulation, the onset of instability occurs and salt is transported into the deep layers of the aquifer. The concentration maximum remains then at a value of around 20 gl^{-1} close to the surface, which is in good agreement with field observations (c.f. section 5.2). In contrast to the simulation without density effects, the variable density simulation can explain, why the central concentration does stabilize and it offers a possible explanation for the deep saline groundwaters found in the Okavango Delta region.

TEM-SURVEYS AND FIELD DATA

Methods

TEM surveys were conducted on several islands in the Okavango Delta to determine the electrical conductivity distribution in the subsurface. The Protem 47D (Geonics Ltd.) instrument was used in the central loop layout (40 m side length in our case). The time domain response was modelled as a standard layered earth response using TEMIX-GL and EMvision software.

The electrical resistivity, *R*, of the formation as measured by electromagnetic techniques is related to the electrical resistivity of the groundwater by Archie's law:

$$R_{form} = R_{water}\, a\, n^{-m} \qquad (12)$$

n is here the porosity and a and m are empirical parameters. Default values for sand are a=1 and m=1.5. Groundwater conductivity and TDS content are correlated, and usually the following rule of thumb is applied:

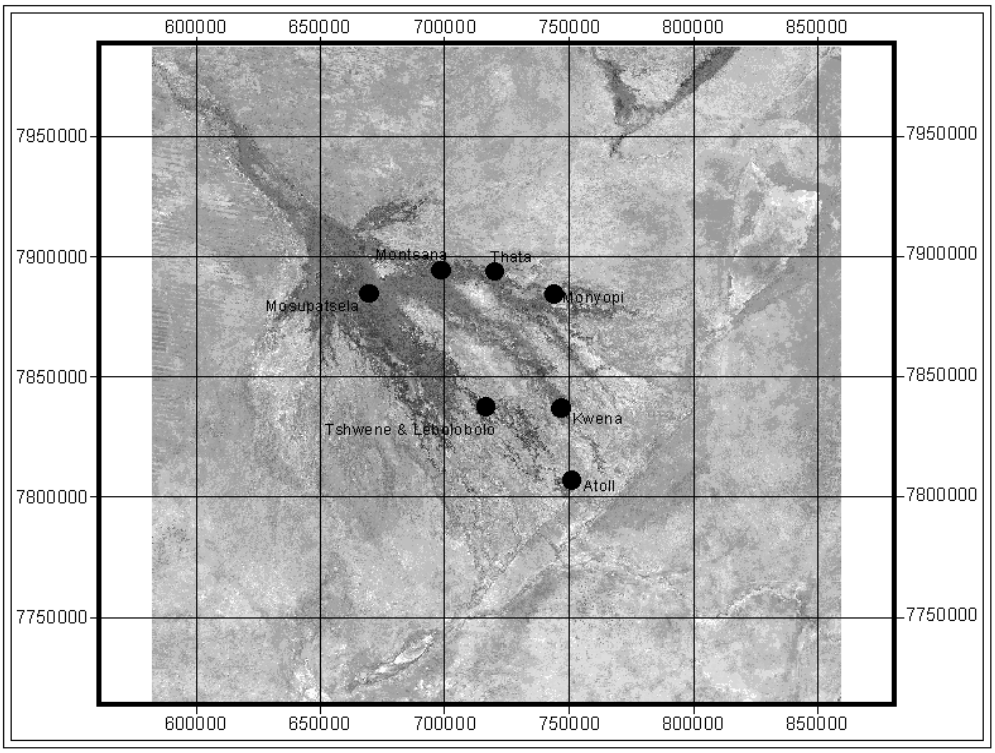

Figure 4 *Locations of the islands. In this and all following maps the projection is UTM Zone 34 S.*

$$TDS\left[\mathrm{mg/l}\right] = 0.65 \cdot \sigma\left[\mu\mathrm{S/cm}\right] \tag{13}$$

The final relationship between TDS and density ρ can be linearized and takes the following form:

$$\rho\left[\mathrm{kg/m^3}\right] = 1000 + 0.7 \cdot TDS\left[\mathrm{kg/m^3}\right] \tag{14}$$

Along with the TEM soundings, the water table and water chemistry on the islands were surveyed. Relative water levels were measured using a Leica theodolite (TC1610) and the electrical conductivity of the water was measured in the field with a conductivity meter (WTW LF 323). Detailed chemical analyses of the samples are underway.

Results

TEM surveys were done on 9 different islands in the Okavango Delta. The locations of these Islands are shown in Figure 4. All of the islands displayed a strong electric conductivity anomaly below their centre. That anomaly could be observed in the TEM data as well as in conductivity samples taken from the shallow groundwater. Pronounced differences were observed with respect to the strength of the anomaly and the maximum concentrations in the island's centre. Some islands such as Monyopi and Montsana displayed only a weak anomaly and maximum electrical conductivity of the groundwater not exceeding 5 $\mathrm{mScm^{-1}}$; whereas islands like Thata, Atoll, Tshwene and Lebolobolo showed extremely strong anomalies with groundwater conductivities exceeding 30 $\mathrm{mScm^{-1}}$.

Furthermore, some islands (e.g., Mosupatsela) are embedded into a regional hydraulic gradient. The maximum concentrations are therefore not observed in the centre of the island but shifted to the downstream side of the island. In the absence of a regional gradient, the concentration maximum is found centrally. Thata and Tshwene islands are examples for this situation.

Apparent Resistivity, water level and groundwater conductivity

The results of TEM surveys, levelling and water table surveys are presented in the following figures for Thata Island. The transects showed a strong conductivity anomaly, which can be clearly seen in the contour-plot of the late apparent resistivity and also in the measured electrical conductivity of the groundwater (Figure 5).

Thata Island is located in the permanent swamp area. The southern part of the island is surrounded by water all the time, whereas the floodplains in the Northern part were dry at the time of the survey. Therefore, the measured transects could extend far out into the floodplains. Groundwater sampling was done in only one borehole for each transect, due to the heavily cemented layers encountered.

Layered earth modelling

Layered earth modelling is employed as a standard technique for the interpretation of TEM soundings. The electromagnetic field is modelled as the response of a half-space consisting of several horizontal layers with a certain homogenous electrical conductivity and a certain thickness. Table 2 shows the results for Transect 1 on Thata Island. Initially the 3-layer model that fitted the data best was calculated. The first layer was postulated to be saline, the second layer fresh and the third layer saline again. In the soundings located out in the floodplains, a first layer was neglected, as there is no reason for superficial build-up of salinity.

In Table 2, the standard fitting error is given in the last column. All parameter combinations having a standard error of up to 10% more than the best-fit model, were calculated here fore. This yielded the confidence intervals for the parameters indicated in Table 2. If the confidence interval was larger than the parameter value itself, it was concluded that the respective parameter couldn't be estimated, as indicated by a dash.

If the resistivity of the first layer was above 3-4 Ω m, the soundings could be satisfactorily fitted and reasonable values for the resistivities and thicknesses resulted. However, in the centre of some islands, resistivities were lower. This had two consequences: First, the maximum exploration depth decreased and no information on the deeper layers could be obtained. The only parameters that could be reliably inferred from the TEM in the centre of the islands were the resistivity and the thickness of the first layer. Thus in the island's centre, where we are most interested in the vertical structure of the conductivity, these TEM data only sample the uppermost layer. Second, the TEM data in the islands' centre could not be satisfactorily fitted by a layered earth response. Figure 6 shows a typical measured profile from the centre of Thata Island, along with the best-fit 3-layer earth model. The 3-layer model cannot reproduce the shape of the curve and an unrealistically high resistivity contrast between the first and the second layer would be calculated (0.4-1400 Ω m). Furthermore, the first layer is calculated to be very thin (0.8 m). Hence, the ascending branch of the sounding could not be interpreted in terms of a layered earth model. For the final interpretation, the ascending branch was therefore masked and only the descending branch was used to calculate the model parameters. This fit is also shown in Figure 6.

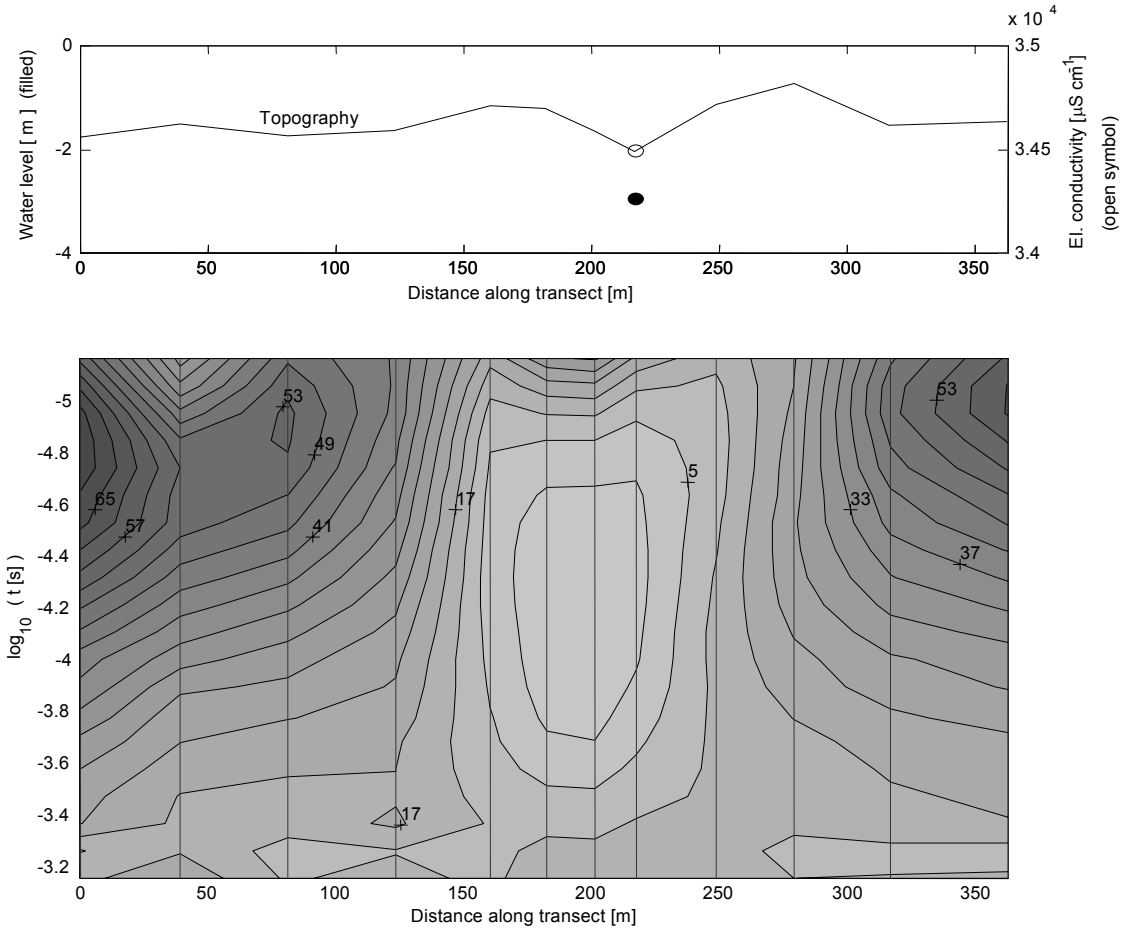

Figure 5 *Theta Island Transect 1 showing topography, water level and electrical conductivity (top), late apparent resistivity [Ωm] (bottom)*

Sounding Location	hor. coord. (m)	Resistivity Layer 1 (ohm-m)	Resistivity Layer 2 (ohm-m)	Resistivity Layer 3 (ohm-m)	Thickness Layer 1 (m)	Thickness Layer 2 (m)	Fitting Error (%)
1	0	23.7 ± 3.0	146.4 ± 20.0	14.0 ± 1.0	2.9 ± 0.6	43.7 ± 2.5	6.1 + 0.61
2	39	6.3 ± 1.0	157.0 ± 60.0	11.0 ± 1.5	1.2 ± 0.2	41.2 ± 4.0	9.9 + 0.99
3	81		61.0 ± 3.0	11.7 ± 0.9	-	39.0 ± 2.1	6.5 + 0.65
4	123		45.0 ± 1.8	17.3 ± 1.0	-	30.0 ±2.6	5.1 + 0.5
5	161	7.5 ± 0.2	31.3 ± 2.6	10.1 ± 1.7	11.5 ± 0.8	73.3 ± 10.4	2.2 + 0.2
6	182	1.8 ± 0.05	-	-	5.5 ± 0.4	-	9.9 + 1.0
7	201	1.7 ± 0.3	-	-	5.6 ± 1.8	-	9.6 + 1.0
8	217	2.3 ± 0.25	-	10.4 ± 4.0	4.8 ± 0.5	83.0 ± 13.0	7.6 + 0.8
9	248	5.0 ± 0.35	52.4 ± 14.5	18.0 ± 2.0	3.0 ± 0.3	26.3 ± 6.4	5.3 + 0.53
10	279	4.3 ± 0.35	68.0 ± 16.0	13.6 ± 0.8	1.2 ± 0.15	29.6 ± 2.0	4.3 + 0.43
11	316		52.4 ± 2.0	13.6 ± 0.8	-	36.0 ± 1.8	5.2 + 0.5
12	363		66.7 ± 2.8	14.3 ± 0.8	-	35.8 ± 1.6	5.3 + 0.5

Table 2 *Thata Island Transect 1*

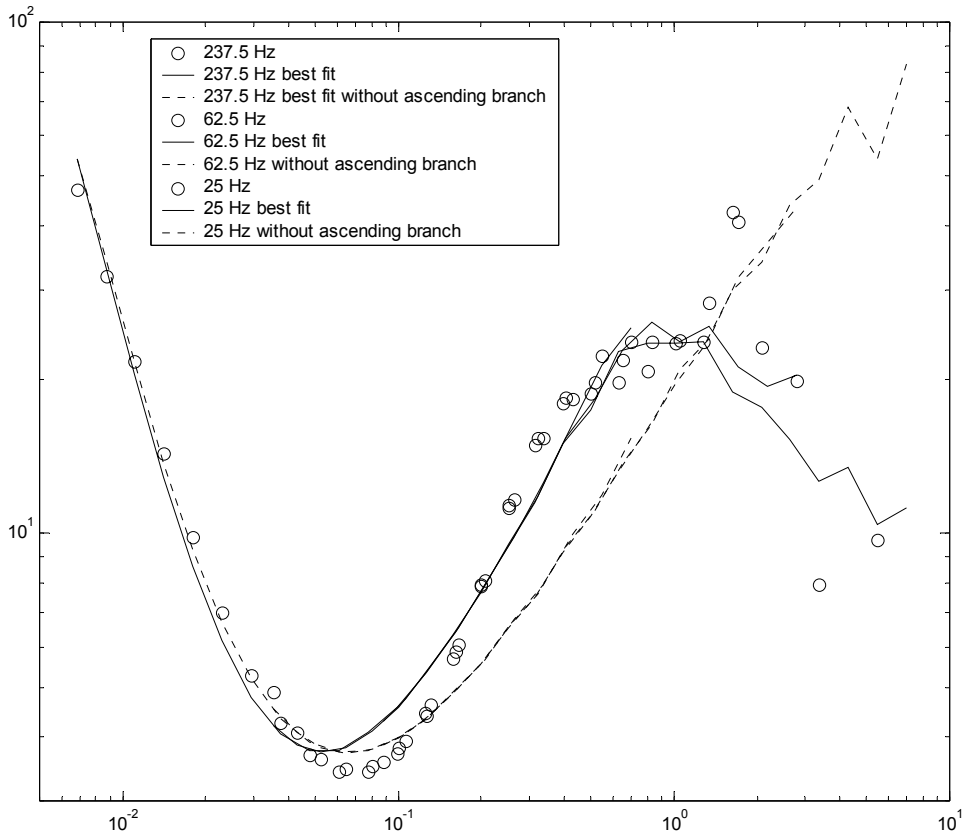

Figure 6 *Measured data and modelling responses for Thata Transect 1 Sounding 7 (see text for explanation)*

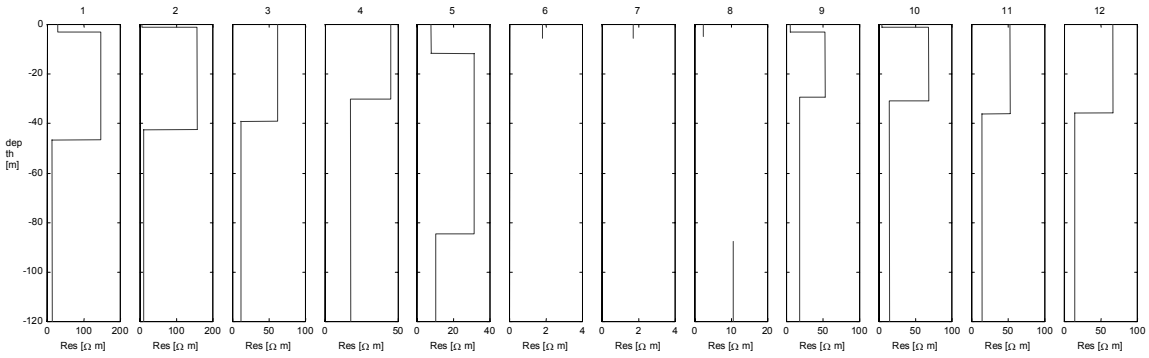

Figure 7 *Modelling results for Thata Island Transect 1*

For islands, where measurements in the floodplains could be made, trends in electrical conductivities and depths are revealed that correspond approximately to the picture derived from the density flow modelling. On all islands, the conductivity and the thickness of the first layer are strongly increasing towards the island centre. Also in the second and third layer, the conductivities increase up to the point where the EM response becomes insensitive to those layers and, consequently, their parameters can no longer be determined (Figure 7). Finally, it is remarkable, that the maximum determined conductivity did not exceed 30-40 $mScm^{-1}$ on any island. If density flow is not taking place, there is no reason, why the concentration should stabilize at such level below the advective-dispersive steady state concentration.

Stability Numbers

The results from the TEM and groundwater surveys were used to obtain an estimate for the Wooding numbers for the investigated islands. First, the formation conductivity of the first layer from the TEM inversion and the measured groundwater conductivity were used to estimate the porosity (Equation 12). Those estimates are rather high. A representative value for the conductivity of the second layer was derived from the soundings outside the islands. That value should reflect the situation in the second layer before the onset of instability. Using Equations 13 and 14, the normalized density contrast between the first and second layer was computed. Taking fixed values for ET and k_f , a Wooding number could thus be calculated.

With an ET-rate of 10^{-8} ms^{-1} and vertical k_f value of 10^{-5} ms^{-1}, the Wooding number for Transect 1 on Thata Island equals 15.2. Such value is supercritical for the onset of vertical, density driven fingering (cp. to critical value of 7.0). The other islands vary in the extent to which salt accumulation has progressed. There are comparatively young islands in terms of salt accumulation, like Monyopi and Montsana, where the concentration maximum in the centre is still low and the Wooding number is sub critical; whereas several islands exhibit supercritical Wooding numbers and inspection of the TEM data hints that density flow may there indeed take place.

CONCLUSIONS

Is density flow balancing the salt budget of the Okavango Delta? Our basic question could still not be resolved fully. However, there is evidence from the large-scale salt balance and from detailed small scale studies on islands, which suggests that density flow may be the dominant balancing mechanism. Still, the here compiled data allow for different interpretations and no salt balancing mechanism could be singled out by field evidence. More data are required and a forthcoming field campaign, which will include DC-resistivity soundings and C-14 dating as well as drilling in the centre of a selected island, may provide distinctive answers to this question.

Nevertheless, our results already allow us to draw conclusions concerning the functioning of the Okavango Delta and its sustainable management. The large-scale arguments presented in this paper clearly show the importance of the micro topographic complexity and length of wetland/dryland interface for keeping the Delta fresh. The large coastline length in the Delta, which is due to the thousands of islands and peninsulas, is a key factor controlling the salt budget. Any human or natural impact altering this situation presents a threat to the chemical equilibrium of the Delta. The high quality of the Okavango waters is one of the principal assets of the region, particularly for the local communities taking their domestic supply either from the surface water itself or from shallow aquifers.

Generally, it can be said that from the upstream to the downstream side of the Delta, a gradual variation of the environment is observed: In the upstream part, isolated high salinity anomalies are found below islands in a generally fresh-water environment. This picture is inverted in the downstream parts: Here we find isolated freshwater lenses along channels in a generally saline environment.

Acknowledgements:

We thank the Department of Water Affairs for highly effective support during field campaigns. The crew of Xaxaba Lodge supplied valuable logistic help on Tshwene and Lebolobolo Islands. The Institute of Applied and Environmental Geophysics at ETH borrowed us the PROTEM D instrument and Hansruedi Maurer gave very helpful advice regarding TEM. We thank the Geological Survey of Austria in Vienna for helping and supplying software during the interpretation of the TEM results.

REFERENCES

Bauer, P., Brunner, P., Kinzelbach, W., 2002**:** Quantifying the net exchange of water between land and atmosphere in the Okavango Delta, Botswana. Proceedings of MODEL CARE 2002, Prague.

Zen, C. and P.P. Wang, 1999: MT3DMS: A modular three-dimensional multi-species model for simulation of advection, dispersion and chemical reactions of contaminants in groundwater systems; Documentation and User's Guide, Contract Report SERDP-99- 1, U.S. Army Engineer Research and Development Center, Vicksburg, MS.

Gieske, A., 1992: Dynamics of Groundwater Recharge. A Case Study in Semi-Arid Eastern Botswana. PhD Thesis, Free University of Amsterdam.

Gumbricht, T., McCarthy, J. and McCarthy, T., 2002: Channels, wetlands and islands in the Okavango Delta, Botswana, and their relation to hydrological and sedimentological processes. Submitted to Earth Surface Processes and Landforms.

Guo, W. and C. D. Langevin, 2002: User's Guide to SEAWAT: A Computer Program for Simulation of Three-Dimensional Variable-Density Ground-Water Flow U.S.Geological Survey, Open-File Report 01-434. Tallahassee, Florida.

McCarthy, J., Gumbricht, T., McCarthy, T.S., Frost, P.E., Wessels, K., Seidel, F., 2002: Flooding Patterns of the Okavango Wetland in Botswana between 1972 and 2000. Submitted to Ambio.

McCarthy, T.S. and Ellery, W.N., 1994: The effect of vegetation on soil and ground water chemistry and hydrology of islands in the seasonal swamps of the Okawango fan, Botswana. Journal of Hydrology, 154:169-193

McDonald, M.G., and Harbaugh, A.W., 1988: A modular three-dimensional finite-difference ground-water flow model: U.S. Geological Survey Techniques of Water-Resources Investigations, book 6, chap. A1, 586 p.

Wooding, R.A., 1960: Raleigh instability of a thermal boundary layer in flow through a porous medium. Journal of Fluid Mechanics, 9:183-192.